Korean J. Chem. Eng., 40(1), 136-144 (2023)
DOI: 10.1007/s11814-022-1243-8

pISSN: 0256-1115
eISSN: 1975-7220

Polyethylenimine-crosslinked calcium silicate hydrate derived from oyster shell waste for removal of Reactive Yellow 2

Su Bin Kang*, Zhuo Wang*, and Sung Wook Won*,,†**

*Department of Ocean System Engineering, Gyeongsang National University,
2 Tongyeonghaean-ro, Tongyeong, Gyeongnam 53064, Korea
**Department of Marine Environmental Engineering, Gyeongsang National University,
2 Tongyeonghaean-ro, Tongyeong, Gyeongnam 53064, Korea
(*Received 11 March 2022 • Revised 20 July 2022 • Accepted 26 July 2022*)

Abstract−Large amounts of oyster shells are often dumped in natural water and landfills, causing pollution and health/sanitation issues. It is highly desirable to convert oyster shell wastes into high-value-added products. In this study, an oyster shell waste-based adsorbent, polyethylenimine-crosslinked synthesized calcium silicate hydrate (PEI/S-CSH), was developed through a two-step processing route consisting of CSH synthesis and PEI crosslinking. The prepared adsorbent was characterized using FT-IR, XRD, BET, FE-SEM, and Zeta potential analyzer, and the results showed that the PEI/S-CSH was successfully prepared. In addition, the adsorption performance of PEI/S-CSH was investigated for a reactive dye, Reactive Yellow 2 (RY2), and adsorption experiments were conducted for variables such as pH value, initial concentration, and time. The PEI/S-CSH removed more than 90% of the initial RY2 concentration in the pH range of 2-7, and was almost unaffected in the NaCl concentration range of 0.01-0.1 M. The maximum RY2 uptake of PEI/S-CSH by the Langmuir model was estimated to be 235.0 and 156.0 mg/g at pH 2 and 7, respectively. The adsorption equilibrium was affected by the pH change and equilibrium was reached within 10 min at pH 2 and 30 min at pH 7. The reusability of PEI/S-CSH was investigated through repeated adsorption/desorption evaluation for a total of five times. As a result, PEI/S-CSH showed good adsorption/desorption performance for RY2 up to five times. Therefore, PEI/S-CSH can be considered as an adsorbent with high potential for removing reactive dyes.

Keywords: Oyster Shell Waste, Recycling, Polyethylenimine, Reactive Yellow 2

INTRODUCTION

The fishing industry has long been an important source of income and food. With the rapid expansion of global aquaculture, oysters in particular have become one of the world's most grown shellfish. According to the Food and Agriculture Organization (FAO), the global production of oysters reached 5.2×10^6 tons in 2015, and the oyster shell waste amounted to nearly 3.9×10^6 tons [1]. Oyster shell waste not only contaminates the soil, groundwater, and aquafarming in coastal areas, but also causes discomfort due to the generation of odors. Although the oyster shell itself is not biodegradable, the organic matter remaining in the oyster shell easily becomes a breeding ground for harmful microorganisms and causes decay by microorganisms [2,3]. In addition, oyster shell waste is more left unattended due to its large volume and lack of proper disposal. To solve this issue, many researchers have tried to develop various technologies for recycling oyster shell wastes as municipal sewage treatment agent [4], cement material [5], agricultural supplement [6], etc., but these technologies are currently far from industrial application. Therefore, there is still a need to find appropriate methods for recycling oyster shell wastes.

†To whom correspondence should be addressed.
E-mail: sungukw@gnu.ac.kr

Oyster shells consist of more than 95% calcium carbonate ($CaCO_3$), a well-known renewable biomineral, and have a hierarchically well-defined structure with adsorption potential [7,8]. Xu et al. [9] evaluated the adsorption of lead, copper, and cadmium by oyster shell powder (OSP), and the maximum adsorption capacity was 26, 8, and 11 mg/g for lead, copper, and cadmium, respectively. Inthapanya et al. [10] investigated the removal efficiency of calcined oyster shells for anionic dye Acid Green 25 and observed a maximum adsorption capacity of 34.1 mg/g at pH 11. He et al. [11] developed a modified oyster shell adsorbent for Hg(II) removal. They found that the removal efficiency of Hg(II) could be improved through modification of the oyster shell. However, the adsorption capacity of the oyster shell-based adsorbents was relatively low. In addition, oyster shells have low acid resistance. These drawbacks limit the use of oyster shells as adsorbents to remove ionic pollutants. Chen et al. [12] succeeded in synthesizing calcium silicate hydrate (CSH) using oyster shells through a calcification strategy, and the synthesized CSH (S-CSH) showed good resistance to acid solutions [12]. However, the adsorption capacity of the S-CSH was still deficient because only hydroxyl groups were present on the S-CSH surface [13]. Since adsorption performance is affected by the surface structure, surface chemical properties, and electrochemical properties of materials, the performance of the adsorbent can be significantly improved through surface modification [14,15].

Polyethylenimine (PEI) is a widely used surface modification agent

owing to its highly branched structure with a large number of amine groups. It can be easily assembled on the surface of various matrix materials to form a single layer to alter the physicochemical properties of the substrate surface [16-19]. In our previous studies, PEI was successfully used to enhance the adsorption capacity of chitin [20] and polyvinyl chloride fiber [21].

Even at low quantities, reactive dyes are extremely hazardous. The introduction of these dyes into water can result in a scarcity of clean water, posing a serious hazard to human life and the environment. Various investigations are needed to remove dyes from wastewater based on these facts. For dye wastewater treatment, several approaches have been used, including filtration, oxidation, photocatalytic degradation, microbiological decomposition, and adsorption [22]. Adsorption is one of the most appealing treatment methods because of its low cost, low formation of harmful by-products, ease of operation, flexibility, and adsorbent reusability [23].

In this study, PEI-crosslinked S-CSH (PEI/S-CSH) was fabricated by cross-linking PEI to the hydroxyl groups on the surface of S-CSH derived from oyster shell waste. The prepared PEI/S-CSH was characterized by Fourier transform infrared spectroscopy (FTIR), X-ray diffraction (XRD), field emission scanning electron microscope (FE-SEM), Brunauer-Emmett-Teller (BET), and Zeta potential analyzer. To examine the adsorption performance of PEI/S-CSH, a representative reactive dye, Reactive Yellow 2 (RY2), was selected as a model dye. RY2 adsorption by PEI/S-CSH was evaluated through various adsorption experiments, such as pH effect, inorganic effect, isotherm, and kinetic experiments. The adsorption-desorption experiment was replicated five times to evaluate the reusability of PEI/S-CSH.

MATERIALS AND METHODS

1. Materials

Oyster shell waste was collected from a local market in Tongyeong, South Korea. Branched PEI (M_w: 70,000, content: 50%) was purchased from Habjung Moolsan Co., Ltd. (Seoul, Korea). Glutaraldehyde (GA, 25% solution, extra pure) was supplied by Junsei Chemical Co., Ltd. (Tokyo, Japan). 3-Aminopropyltriethoxysilane (APTES, 99%) was provided by Daejung Chemical & Metals Co., Ltd. (Siheung, Korea). RY2 and fumed silica were purchased from Sigma-Aldrich Korea Ltd. (Yongin, Korea). Typical properties of RY2 include a color index number of 18972, a maximum absorption wavelength (λ_{max}) of 404 nm, a dye content of 65%, a molecular formula of $C_{25}H_{15}Cl_3N_9Na_3O_{10}S_3$, and a molecular weight of 873.0 g/mol. Other reagents, such as toluene, NaOH, and HCl used in this study, were of analytical grade.

2. Preparation of PEI/S-CSH

Oyster shell wastes were first washed with water several times to remove impurities and sediment, and air-dried for one day. The washed oyster shells were soaked in 5% sodium hypochlorite (NaClO) solution for 24 h to get rid of organic matter attached on the surface, then washed with distilled water and dried completely. The dried oyster shells were crushed by a ball mill (DW BM915, Dongwon scientific system co., Korea) with alumina balls at 500 rpm to produce oyster shell powder (OSP). The OSP with a particle size of less than 90 μm was collected through sieving. A mixture of OSP and fumed silica with a weight ratio of 1 : 1.4 was calcined at 800 °C for 2 h, followed by hydrothermal treatment at 150 °C for 12 h to obtain S-CSH [12].

PEI/S-CSH was prepared based on previously reported methods with slight modifications [19]. Briefly, S-CSH (3 g) and APTES (3.75 mL) were added to 300 mL of toluene and stirred at room temperature for 16 h. Then, the APTES treated S-CSH was collected by filtration, washed with ethanol several times, and dried overnight at 100 °C. Thereafter, after treatment with 5% GA solution (75 mL) at room temperature for 1 h, it was sequentially washed with excess deionized water and acetone, and dried in an oven at 100 °C for 2 h. Finally, PEI/S-CSH was produced by mixing 1% PEI solution at room temperature for 24 h. The obtained PEI/S-CSH was washed with deionized water several times, dried in an oven at 40 °C for 24 h, and stored in a desiccator for further use. The color change of representative samples by stage is shown in Fig. S1. The structure of the PEI/S-CSH was presented in Scheme 1.

3. Analytical Methods

The IR spectra of OSP, S-CSH, and PEI/S-CSH were investigated in the range of 4,000-400 cm^{-1} using a FTIR spectrometer (4000 series, Jasco, Japan). The specimens for FTIR analysis were arranged in the form of pellets by uniformly mixing the adsorbent and KBr reagent and compressing the mixture. The composition of OSP, S-CSH, and PEI/S-CSH was analyzed using XRD (D8 Advance A25, Bruker, USA) with Cu Kα radiation (λ=1.54 Å) and 2θ range from 10° to 70°. Nitrogen adsorption-desorption isotherms of S-CSH and PEI/S-CSH were collected using 3Flex surface characterization analyzer (Micromeritics, USA). The surface morphology of OSP, S-CSH, and PEI/S-CSH was observed by FE-SEM (JSM-7610F, Jeol, Japan) at 15,000x magnification. The zeta-potential of S-CSH and PEI/S-CSH at different pH values was analyzed using a zeta-potential analyzer (ELSZ-2000, Otsuka, Japan).

4. Batch Adsorption and Desorption Experiments

A stock solution of the hydrolyzed RY2 dye was prepared by dissolving an appropriate amount of RY2 in 0.1 M NaOH and hydrolyzing at 90 °C for 3 h. After cooling to room temperature, the pH of the stock solution was adjusted to 7 using 5 M HCl, and the dye concentration was adjusted to 1,000 mg/L by adding distilled water. The stock solution was diluted with distilled water as needed.

For all batch experiments, 0.03 g of adsorbent and 30 mL of RY2 solution were placed in a 50-mL conical tube and stirred in a shaking incubator at 25 °C and 160 rpm. The effect of pH on dye adsorption by PEI/S-CSH was evaluated in the pH range of 2 to 12 at an initial RY2 concentration of 100 mg/L. The effect of ionic salt on dye adsorption by PEI/S-CSH was performed in a dye solution containing 100 mg/L of RY2. The concentration of NaCl in the dye solution ranged from 0 to 0.1 mol/L. The adsorption isotherm experiments were conducted at pH 2 and 7, respectively, in the RY2 concentration from 0 to 600 mg/L. After reaching equilibrium, samples were collected from the supernatant to analyze the final dye concentration. The adsorption kinetic experiments were conducted using 100 mg/L of RY2 solution at pH 2 and 7, and samples were collected at predetermined time intervals up to 120 min. The samples were centrifuged at 10,000 rpm for 10 min, and the dye concentration remaining in the supernatant was measured using a UV-Vis spectrophotometer (X-ma 3000, human, Korea). The dye uptake, q (mg/g) was calculated using Eq. (1).

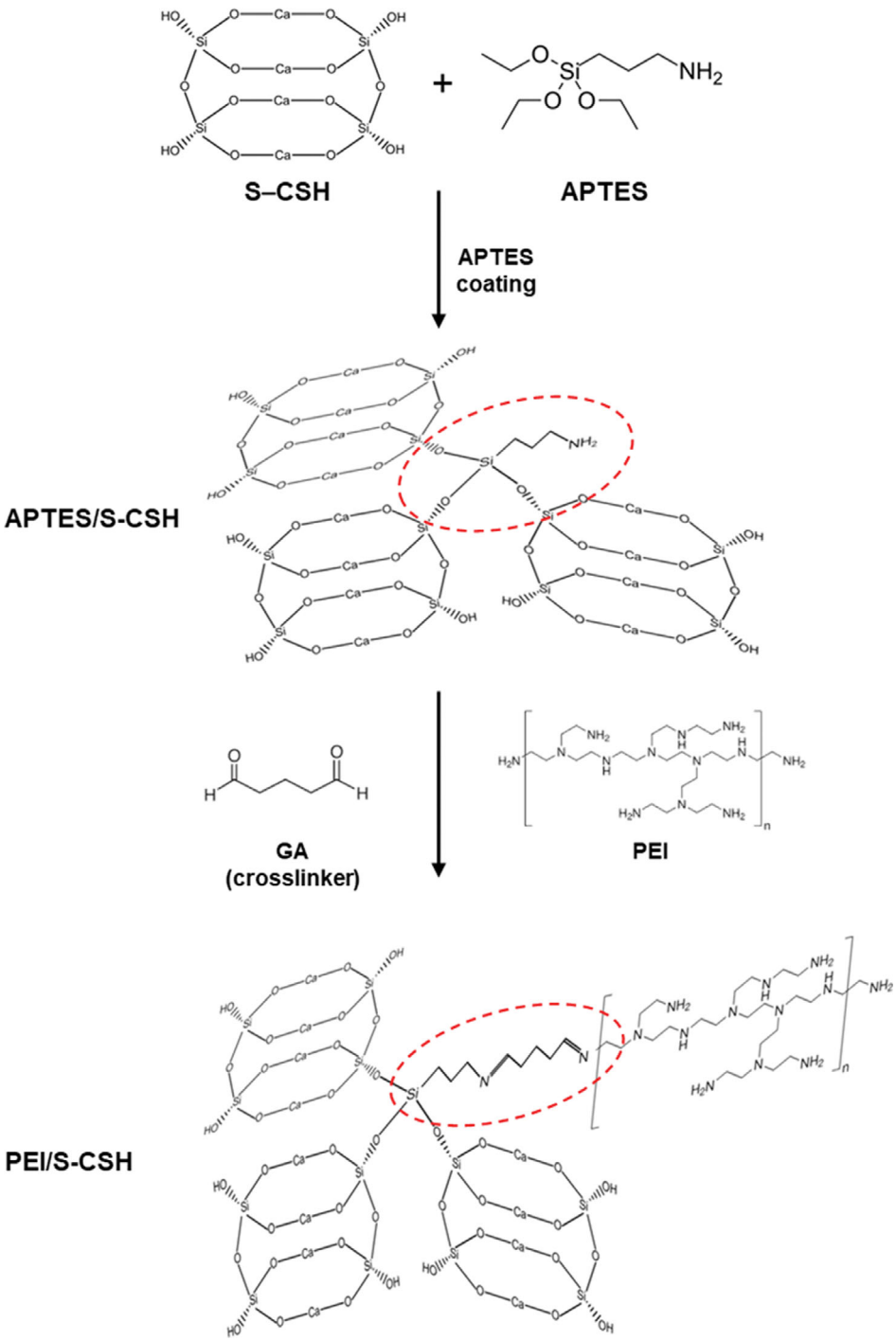

Scheme 1. The structure of the material and the proposed adsorption mechanism.

$$q = \frac{(C_i - C_f)V}{m} \quad (1)$$

where the initial and final RY2 concentrations are expressed by C_i and C_f (mg/L), respectively, the working volume is indicated by V (L), and the weight of the adsorbent is marked by m (g).

For desorption evaluation, RY2-loaded PEI/S-CSH was obtained by mixing PEI/S-CSH with 100 mg/L RY2 solution at pH 2. Then, the RY2-loaded adsorbent was washed with distilled water three times and eluted using 0.01 mol/L NaOH solution. After desorption, the PEI/S-CSH was washed using distilled water for three times and subject to the next adsorption process. The adsorption-desorption experiment was repeated five times to confirm the reusability of the adsorbent. The desorption efficiency was calculated using Eq. (2).

$$\text{Desorption efficiency (\%)} = \frac{\text{Released dye weight (mg)}}{\text{Initially adsorbed dye weight (mg)}} \times 100 \quad (2)$$

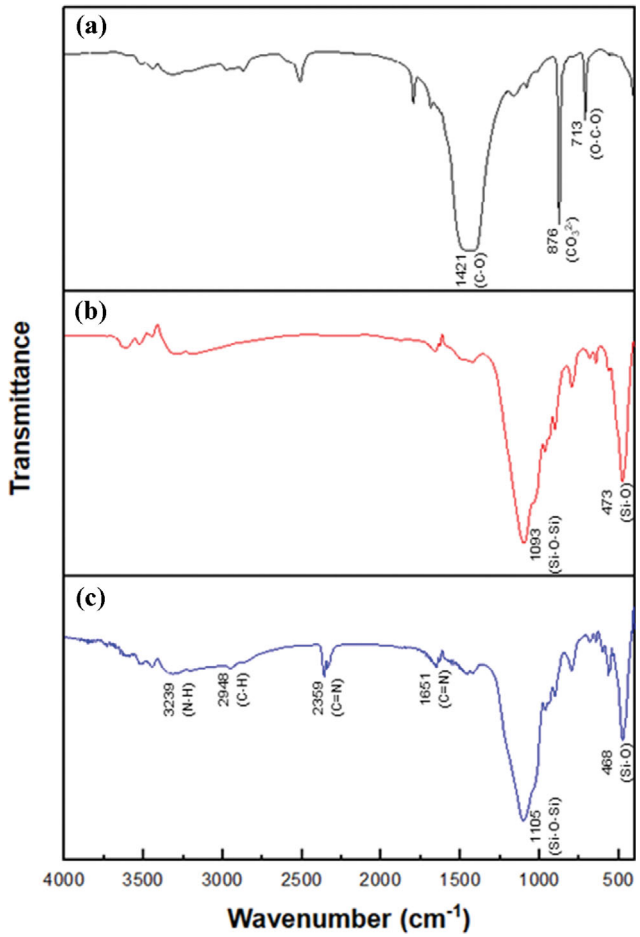

Fig. 1. FTIR spectra of (a) OSP, (b) S-CSH, and (c) PEI/S-CSH.

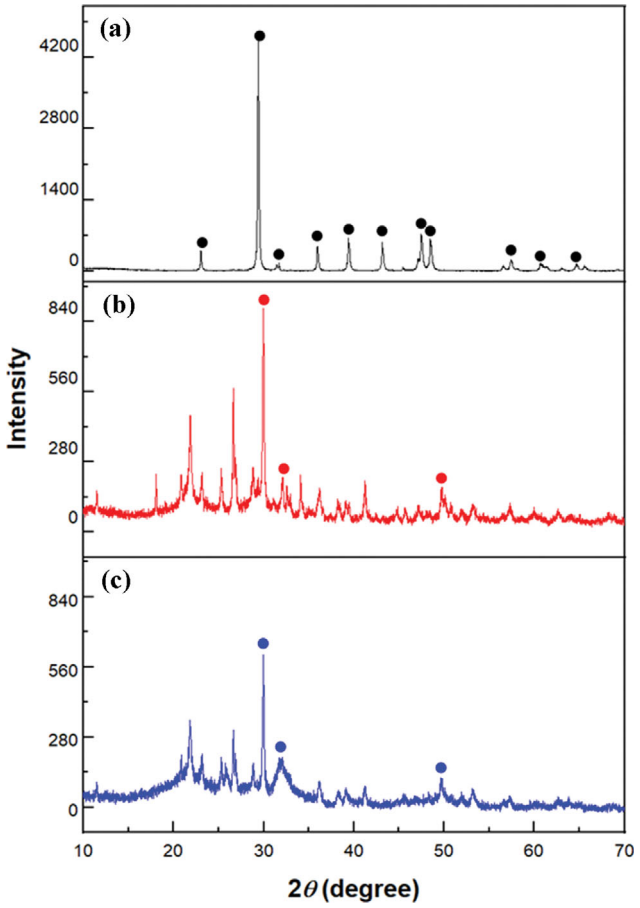

Fig. 2. X-ray diffraction patterns of (a) OSP, (b) S-CSH, and (c) PEI/S-CSH.

RESULTS AND DISCUSSION

1. Characterization

Phase-by-step chemical bond changes in manufactured adsorbents can be investigated by FT-IR spectrometer. The FT-IR spectra of OSP, S-CSH, and PEI/S-CSH are presented in Fig. 1. The main component of OSP is calcium carbonate, and the characteristic peaks of calcite were observed at 1,421 (asymmetric C-O stretching), 876 (CO_3^{2-}-bending), and 713 cm^{-1} (O-C-O bending), respectively [24] (Fig. 1(a)). After being combined with SiO_2, two new strong peaks appeared at 1,093 (Si-O-Si) and 473 (Si-O) cm^{-1} [25], as observed in Fig. 1(b). In addition, the peak of carbonation (CO_3^{2-}-bending) disappeared in the OSP, which appears to be due to decomposition during the calcination at 800 °C. Typically, S-CSH has an -OH group on its surface due to water molecules. After drying treatment, no characteristic peak of hydroxyl group appeared in the range of 3,000-3,600 cm^{-1} [26]. After PEI coating, a broad peak at 3,239 cm^{-1} assigned to the N-H stretching vibration of amine groups [27] was observed as given in Fig. 1(c). The intensity of the peak at 2,948 cm^{-1}, assigned to the C-H stretching vibration of GA and PEI backbone, was enhanced [28], and new peaks were observed at 2,359 and 1,651 cm^{-1}, which were attributed to the stretching vibration of C=N, indicating that the APTES and PEI were successfully crosslinked by GA [29]. Furthermore, Fig. S2 shows an increase in adsorption amount of RY2 from 5.48 to 233.33 mg/g after PEI modification, which is sufficient to support that PEI/S-CSH was successfully prepared.

The mineralogical compositions of OSP, S-CSH, and PEI/S-CSH, as shown in Fig. 2, were determined by XRD analysis. The OSP have a highly crystal structure and the XRD pattern (Fig. 2(a)) is almost identical to that of calcium carbonate (JCPDS card 47-1743) [30]. In contrast, in the XRD pattern (Fig. 2(b)) of S-CSH, several new main peaks assigned to Ca-Si-OH were observed at 2θ= 29.9°, 32.0°, and 49.6°, respectively (JCPDS card 33-0306) [31]. In addition, as shown in Fig. S3, the S-CSH consisted of more than 45% β-wollastonite (JCPDS card 01-075-1396) [32,33]. The structure of β-wollastonite was formed by calcining the mixture of OSP and fumed silica at 800 °C [34]. In addition, the different ratios of Ca, Si, O, and H_2O in the structure make various types of CSH exist. Fig. S4 shows the results of SEM-EDX analysis of PEI/S-CSH. As a result, PEI/S-CSH is composed of Ca, Si, and O due to CSH, the matrix of the adsorbent, which is consistent with the XRD results. The decrease in the diffraction intensities of the characteristic peaks of calcite and S-CSH in PEI/S-CSH can be attributed to the grafting of PEI to the S-CSH surface.

Fig. 3(a) shows the N_2 adsorption-desorption isotherms of S-CSH and PEI/S-CSH. The isotherms of S-CSH and PEI/S-CSH are typical type IV isotherm with H3 hysteresis loops, which are associ-

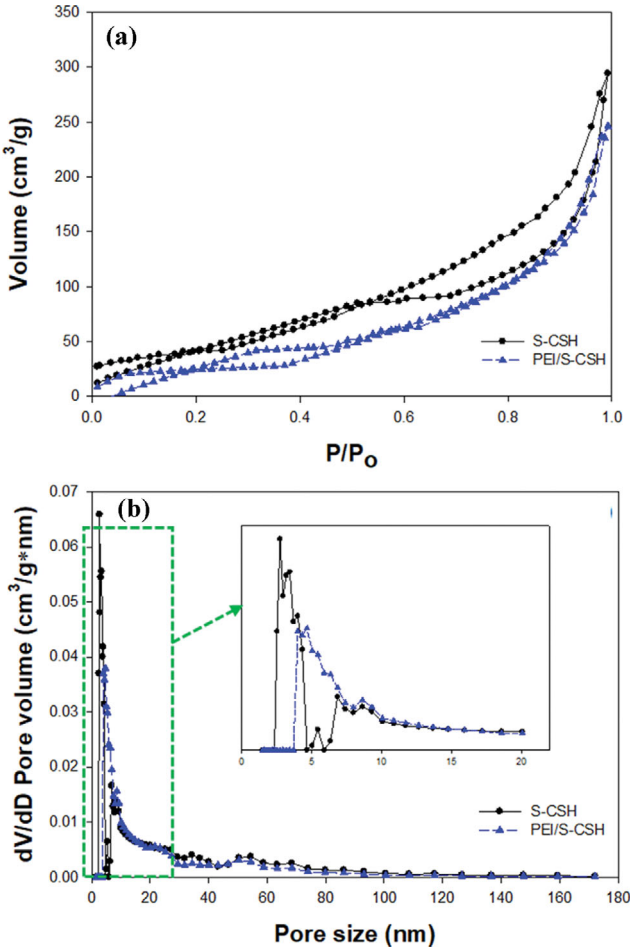

Fig. 3. (a) Nitrogen adsorption-desorption isotherms and (b) BJH-desorption pore size distribution curves of S-CSH and PEI/S-CSH. The inset is enlarged the detail in region of 0 to 20 nm.

Table 1. Parameters of the porous structure of S-CSH and PEI/S-CSH

	Specific surface area (m^2/g)	Volume of pores (cm^3/g)	Average pore size (nm)
S-CSH	212.74	0.284	5.35
PEI/S-CSH	87.38	0.265	12.13

ated with mesopores formed due to aggregation of plate-like particles [35,36]. Fig. 3(b) shows the pore size distribution of S-CSH and PEI/S-CSH. As listed in Table 1, the BET specific surface area of S-CSH and PEI/S-CSH was 212.74 and 87.38 m^2g^{-1}, respectively. In addition, the average pore size increased from 5.35 to 12.13 nm. The decrease in specific surface area could be due to the pores of about 4 nm or smaller being covered after PEI grafting. At the same time, due to the aggregation of S-CSH nanoparticles, new, larger pores were created, so the average pore diameter was increased.

The microstructure of OSP, S-CSH and PEI/S-CSH showed remarkable differences in size and shape (Fig. 4). In general, OSP was observed in angular form [37,38], but the OSP used in experiments was crushed by ball-mill, so the angular and rounded parts

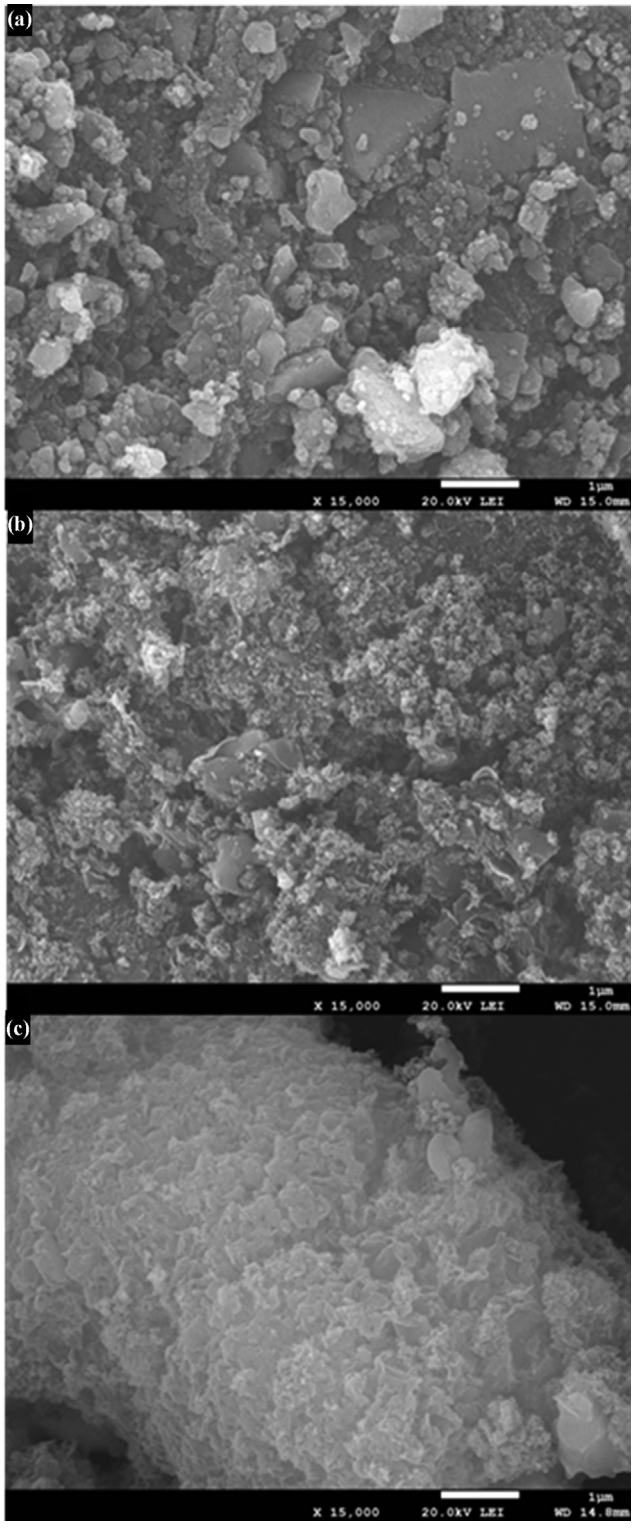

Fig. 4. FE-SEM images of (a) OSP, (b) S-CSH and (c) PEI/S-CSH at 15,000x magnification.

coexist. After synthesis into S-CSH, the overall particle size decreased. Fig. 4(c) shows a very interesting appearance after the PEI coating. The particles are clustered and have a form that seems to be stacked in layers. These surface changes confirm that the step-by-step materi-

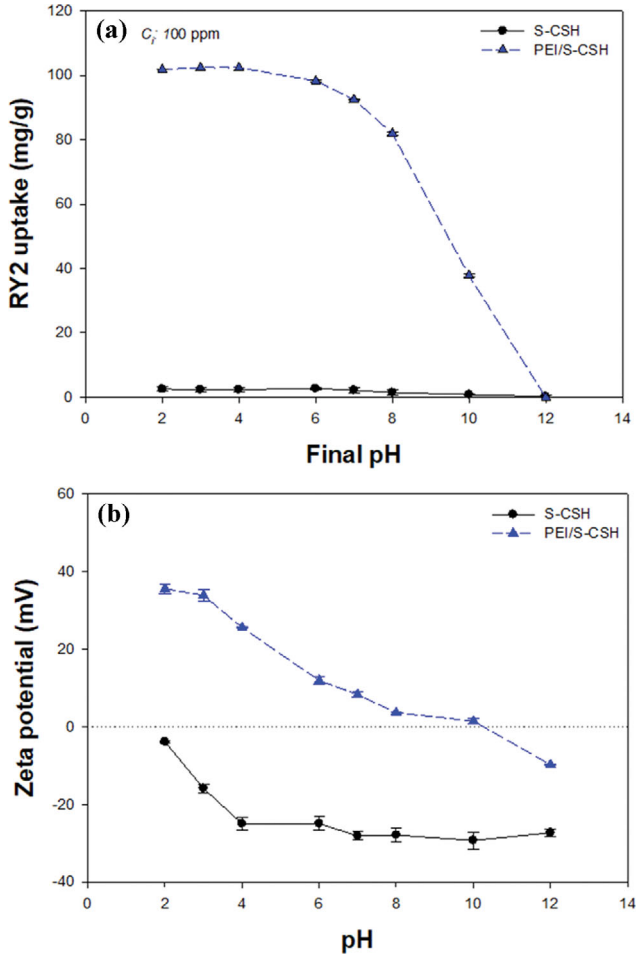

Fig. 5. (a) Effect of pH value on the adsorption of RY2 by PEI/S-CSH (Experimental conditions: pH value, 1-12; volume of solution, 30 mL; mass of adsorbent, 30 mg; initial RY2 concentration, 100 mg/L) and (b) Surface zeta potential of S-CSH and PEI/S-CSH with different pH value.

als are well-modified. Besides, it helps to understand XRD and BET analysis results.

2. pH Effect

The pH of solution is an important parameter in dye adsorption research because it can change the ionization degree of the adsorbate as well as the surface control process of the adsorbent. The influence of pH on RY2 uptake was investigated in the pH range of 2-12, and the result is shown in Fig. 5(a). The S-CSH did not adsorb RY2 in the overall pH range. On the contrary, the adsorption capacity of the PEI/S-CSH for RY2 decreased with increasing the pH value. As a result, the removal rate of RY2 was 100% in the pH range of 2-4. After pH 6, the removal rate gradually decreased and dropped sharply after pH 8. Furthermore, adsorption barely occurred at pH 12.

Adsorbents can interact with ionic pollutants through electrostatic attraction or repulsion, and these interactions depend on the pK_a value present on the adsorbent surface [39]. According to the experiment result, the pK_a of PEI/S-CSH may be affected by PEI present on the surface. The branched PEI used in this experiment

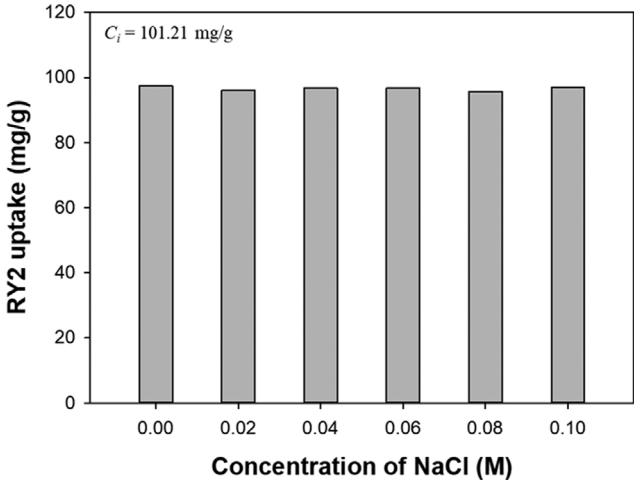

Fig. 6. Effect of ionic salt on the adsorption of RY2 by PEI/S-CSH (Experimental conditions: pH value, 2; volume of solution, 30 mL; mass of adsorbent, 30 mg; initial RY2 concentration range: 100 mg/L; NaCl concentration: 0-0.1 M).

consists of primary, secondary, and tertiary amines, and their pK_a values are 4.5, 6.7 and 11.6, respectively [40].

According to Fig. 5(b), the zeta potential of S-CSH and PEI/S-CSH decreased from −3.85 to −27.29 mV and 35.61 to −9.74 mV, respectively, with the pH value increasing from 2 to 12. The isoelectric point (pH_{IEP}) of S-CSH was lower than 2.0, while that of the PEI/S-CSH was 10.33. When the pH is lower than 10.33, the surface of PEI/S-CSH has positive charge, and at pH>pH_{IFP}, the surface of adsorbent has negative charge. Therefore, the positively charged amine groups (-NH^+, -NH_2^+, NH_3^+) in PEI are likely to be bound with the negatively charged sulfonic groups (-SO_3^-) in RY2 molecules by the electrostatic interaction (Scheme 1) [41]. Based on these results, pH 2 and 7 were selected for future adsorption experiments.

3. The Effect of Ionic Salt

Industrial dye wastewater often contains various kinds of coexisting ions such as Na^+, K^+, Ca^{2+}, SO_4^{2-}, NH_4^+, NO_3^-, and Cl^-. Their ionic strength can influence the adsorption of dyes onto adsorbents. In this study, NaCl was selected as the representative of coexisting ions to evaluate the effect of ionic strength on the adsorption of RY2 by PEI/S-CSH. A dye solution containing 100 mg/L of RY2 was used for this experiment, and the NaCl concentration was in the range of 0-0.1 mol/L. Fig. 6 shows the effect of NaCl concentration on RY2 removal in dye solution. Even when the NaCl concentration was increased from 0 to 0.1 mol/L, the removal efficiency of RY2 was almost the same as 100%. This result indicates that the chloride ions do not significantly compete with the sulfonate groups of the RY2 molecule for the amine sites in the PEI/S-CSH [40].

4. Adsorption Isotherms and Modeling

Adsorption isothermal experiments were performed at pH 2 and 7 to evaluate the maximum adsorption capacity of PEI/S-CSH for RY2. The Langmuir and Freundlich models were used to fit the experimental data, and the results are displayed in Fig. 7. As shown in Fig. 7, the RY2 uptake by the PEI/S-CSH at pH 2 and 7 was increased with the increase of RY2 concentration before attaining the maximum adsorption capacity. The non-linear forms of the Lang-

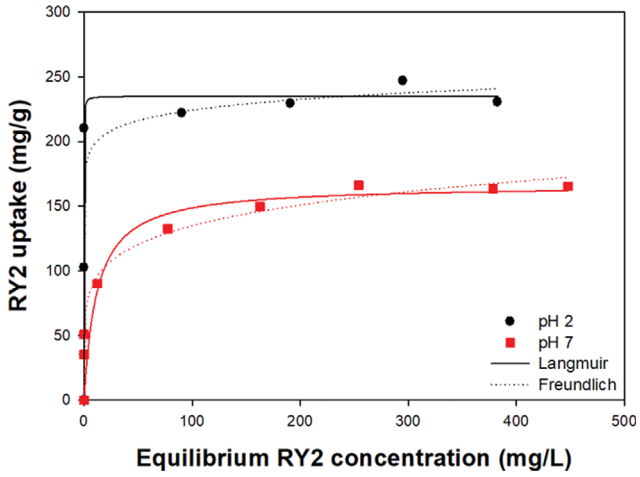

Fig. 7. The Langmuir and Freundlich isotherm models for RY2 adsorption onto PEI/S-CSH (Experimental conditions: pH value, 2 and 7; volume of solution, 30 mL; mass of adsorbent, 30 mg; initial RY2 concentration range, 50-600 mg/L).

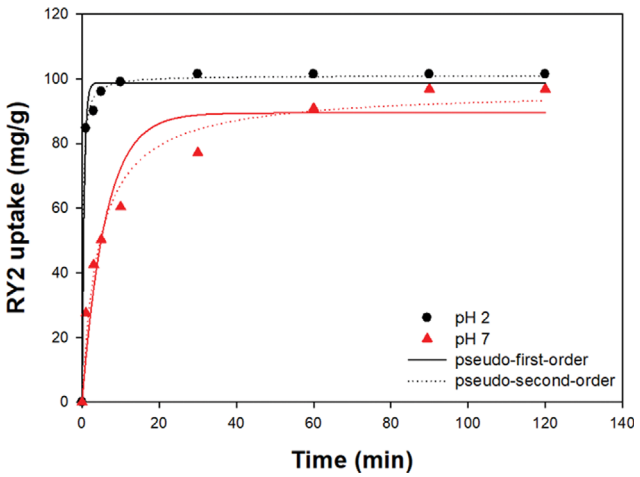

Fig. 8. Pseudo-first- and pseudo-second-order kinetic models for RY2 adsorption onto PEI/S-CSH (Experimental conditions: pH value: 2 and 7; volume of solution, 30 mL; mass of adsorbent, 30 mg; initial RY2 concentration, 100 mg/L).

muir and Freundlich models can be expressed as:

$$\text{Langmuir model: } q_e = \frac{q_{max} b_L C_e}{1 + b_L C_e} \quad (3)$$

$$\text{Freundlich model: } q_e = K_F C_e^{1/n} \quad (4)$$

where q_e (mg/g) represents the amount of RY2 adsorbed at equilibrium, C_e (mg/L) represents the residual concentration of RY2, and q_{max} (mg/g) is the maximum adsorption amount. b_L (L/g) is Langmuir constant which is related to the adsorption free energy. K_F (L/g) and n are Freundlich constant and Freundlich exponent, respectively.

The Langmuir and Freundlich parameters are summarized in Table 2. The coefficient (R^2) values of the Langmuir model were larger than those of the Freundlich model. Besides, the maximum uptake was estimated at 235.00 and 156.01 mg/g at pH 2 and 7, respectively, which was more consistent with experimental results (230.33 and 165.32 mg/g). These results indicate that the Langmuir model was more suitable for describing the adsorption isotherm and the adsorption of PEI/S-CSH for RY2 was monolayer adsorption [20]. The maximum adsorption capacity at pH 2 was approximately 80 mg/g higher than that at pH 7, which was because the adsorbent provides more positively charged binding sites under acidic conditions, as demonstrated by zeta potential analysis (Fig. 5(a)). The Langmuir constant at pH 2 was larger than that at pH 7, implying that PEI/S-CSH has higher adsorption affinity at pH 2 than at pH 7. The Freundlich exponents were above 1, suggesting that the adsorption of RY2 on PEI/S-CSH was favorable. Besides, the Freundlich exponent at pH 2 was higher than that at pH 7, indicating that pH 2 was more favorable than pH 7 for the adsorption of RY2 on PEI/S-CSH.

The maximum adsorption amount of PEI/S-CSH for RY2 was 235.00 mg/g, much higher than that of OSP (16.45 mg/g) and S-CSH (5.48 mg/g) (Fig. S3). In addition, the adsorption capacity of PEI/S-CSH for dye contaminant was compared with several other $CaCO_3$-based biosorbents published in the literature. The adsorption capacity of calcined OS for acid green 25 was 29.2 mg/g [10], *Cerastoderma lamarcki* shell for basic green 4 was 35.84 mg/g [42], scallop shell for reactive black 5 was 90.9 mg/g [43], ground eggshell for acid orange 51 was 113.6 mg/g [44]. The result revealed that the PEI/S-CSH adsorbent prepared in this study is a more promising and excellent adsorbent for dye removal.

5. Adsorption Kinetics and Modeling

Adsorption kinetics is one of the important factors that determine the efficiency of the entire adsorption process as well as providing theoretical insights into the reaction paths and mechanisms of adsorption [45]. The effect of contact time was evaluated in order to find the equilibrium time of RY2 adsorption on PEI/S-CSH. The experiments were performed for 120 min at 25 °C with an initial RY2 concentration of 100 ppm and acidic (pH=2) and neural (pH=7) conditions. As shown in Fig. 8, PEI/S-CSH adsorbed 95% of the RY2 in the acidic condition within the first 10 min and reached equilibrium at 30 min, showing a very fast adsorption rate. In the neutral condition, approximately 90% of the RY2 molecules was ad-

Table 2. Isotherm parameters of RY2 adsorption onto PEI/S-CSH

pH	Langmuir model			Freundlich model		
	q_{max} (mg/g)	K_L (L/mg)	R^2	K_F (L/g)	n	R^2
2	235.00	22.14	0.932	175.49	18.84	0.888
7	156.01	18.84	0.878	97.11	11.44	0.856

Table 3. Kinetic parameters of RY2 adsorption onto PEI/S-CSH

pH	Pseudo-first-order			Pseudo-second-order			
	q_1 (mg/g)	k_1 (L/min)	R^2	q_2 (mg/g)	k_2 (g/(mg·min))	h (mg/g·min)	R^2
2	98.76	1.90	0.988	101.03	0.0449	458.30	0.997
7	89.41	0.17	0.929	96.58	0.0024	22.39	0.974

sorbed within 60 min before reaching equilibrium at about 90 min. Both conditions showed fast adsorption rates, which can be attributed to the large number of active adsorption sites on the surface of PEI/S-CSH.

Equilibrium adsorption data is described by the pseudo-first-order and pseudo-second-order kinetic models. The non-linear forms of these models are expressed as follows:

$$\text{Pseudo-first-order kinetic model: } q_t = q_1(1-\exp(-k_1 t)) \quad (5)$$

$$\text{Pseudo-second-order kinetic model: } q_t = \frac{q_2^2 k_2 t}{1+q_2 k_2 t} \quad (6)$$

where q_t (mg/g) represents the RY2 uptake at time t, and q_1 and q_2 (mg/g) represent the RY2 uptake at equilibrium. k_1 (L/min) and k_2 (g/mg·min) are the rate constants of pseudo-first- and pseudo-second-order kinetic models, respectively. The initial sorption rate, h (mg/g·min), at $t \rightarrow 0$ is defined as Eq. (7):

$$h = k_2 q_2^2 \quad (7)$$

The parameters of kinetic models as well as R^2 values and h are presented in Table 3. The R^2 values of PEI/S-CSH of the pseudo-second-order model were 0.997, and 0.974 at pH 2 and 7, respectively, which were higher than those (0.988 and 0.929) of the pseudo-first-order model. In addition, the q_2 values calculated at pH 2 and pH 7 were closer to the experimental result q_{exp} (101.37 and 96.81 mg/g). These facts revealed that the pseudo-second-order model can predict the adsorption behavior well throughout the whole adsorption process. The pseudo-second-order model constant at pH 2 was higher than that at pH 7, indicating that the adsorption of PEI/S-CSH for RY2 was more favorable at pH 2 than at pH 7. Furthermore, the h value of PEI/S-CSH at pH 2 was calculated to be 458.30 mg/g·min, which is 20.4 times higher than that at pH 7 (22.46mg/g·min), indicating that the pH of RY2 solution affects the initial adsorption rate. It was also confirmed that PEI/S-CSH had a faster initial adsorption rate than other sorbents such as calcined OS (3.95 mg/g·min) [10], C. shell (5.13 mg/g·min) [42], scallop shell (1.70 mg/g·min) [43], and ground eggshell (38.75 mg/g·min) [44]. This is because PEI coating can highly enhance the adsorption rate by introducing more ligand-binding sites on the adsorbent surface, which is highly affected by specific surface areas of adsorbent [46].

6. Reusability of PEI/S-CSH

The reusability of adsorbents is very important for obtaining economic benefit and to prolong the replacement cycle of adsorbents. The RY2-loaded PEI/S-CSH was prepared at an initial RY2 concentration of 100 ppm at pH 2. Then, the RY2-loaded PEI/S-CSH was washed with distilled water and subjected to the desorption process. Considering PEI/S-CSH showed negligible adsorption for RY2 at pH 12 (Fig. 5), the desorption experiment was conducted at pH 12. The adsorption-desorption cycle was repeated five times and the results are depicted in Fig. 9. After five cycles, the adsorption and desorption efficiencies of PEI/S-CSH remained at 98.09% and 98.76%, respectively. As can be seen from the SEM-EDX analysis (Fig. S4), this result indicates that the adsorbent is stably maintained during the adsorption and desorption processes. Furthermore, both adsorption and desorption reached equilibrium within 30 min. The reusability test demonstrated the good chemical stability and high regeneration efficiency of PEI/S-CSH, and this result may help support the long-term application of PEI/S-CSH in water treatment.

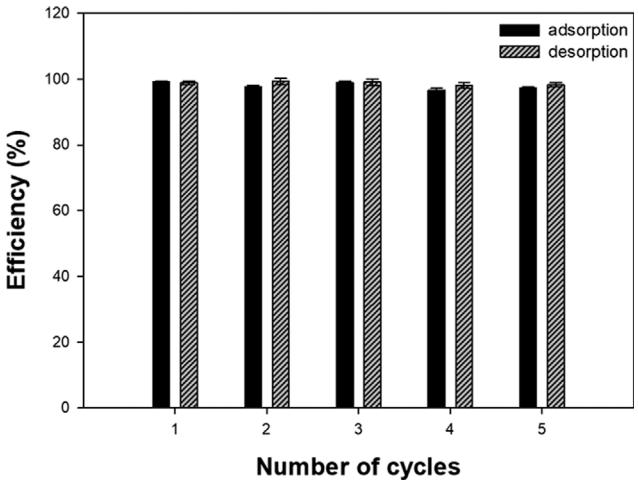

Fig. 9. Repeated adsorption-desorption of RY2 on PEI/S-CSH in a batch process (adsorption conditions: pH value: 2; volume of solution, 30 mL; mass of adsorbent, 30 mg; initial RY2 concentration, 100 mg/L, desorption conditions: pH value: 12; volume of solution, 30 mL; mass of RY2 loaded adsorbent, 30 mg).

CONCLUSION

An oyster waste-based adsorbent, PEI/S-CSH, was developed, providing an alternative for oyster shell waste recycling. FT-IR, XRD, BET, FE-SEM, and Zeta potential analysis revealed that the adsorbent was successfully prepared. The pH edge experiment demonstrated that the PEI/S-CSH was able to adsorb RY2 in a wide pH range (2–7). The Langmuir model was more suitable for depicting adsorption of RY2 on PEI/S-CSH, and the maximum adsorption amount was 235.00 and 156.01 mg/g at pH 2 and 7, respectively. Kinetic experiments showed that the adsorption equilibrium for 100 ppm RY2 at pH 2 and 7 was reached within 10 and 30 min, respectively. Furthermore, PEI/S-CSH can be reused at least five

times according to the reusability study. Overall, the PEI/S-CSH, fabricated from oyster shell waste, showed the possibility of eliminating anionic dye from wastewater.

ACKNOWLEDGEMENTS

This research was supported by Basic Science Research Program through the National Research Foundation of Korea (NRF) funded by the Ministry of Education (NRF-2020R1A6A3A13068967 and NRF-2020R1F1A1065937).

SUPPORTING INFORMATION

Additional information as noted in the text. This information is available via the Internet at http://www.springer.com/chemistry/journal/11814.

REFERENCES

1. M. Bonnard, B. Boury and I. Parrot, *Environ. Sci. Technol.*, **54**(1), 26 (2020).
2. Y. Li, P. Huang, S. Guo and M. Nie, *J. Clean. Prod.*, **272**, 122694 (2020).
3. R. Liu, D. Chen, X. Cai, Z. Deng and Y. Liao, *J. Clean. Prod.*, **266**, 121729 (2020).
4. T.-C. Hsu, *J. Hazard. Mater.*, **171**(1-3), 995 (2009).
5. I. Chiou, C. Chen and Y. Li, *Constr. Build. Mater.*, **64**, 480 (2014).
6. C. H. Lee, D. K. Lee, M. A. Ali and P. J. Kim, *Waste Manage.*, **28**(12), 2702 (2008).
7. Q. Wu, J. Chen, M. Clark and Y. Yu, *Appl. Surf. Sci.*, **311**, 264 (2014).
8. D. Ding, Y. Zhao, S. Yang, W. Shi, Z. Zhang, Z. Lei and Y. Yang, *Water Res.*, **47**(7), 2563 (2013).
9. X. Xu, X. Liu, M. Oh and J. Park, *Pol. J. Environ. Stud*, **28**(4), 2949 (2019).
10. X. Inthapanya, S. Wu, Z. Han, G. Zeng, M. Wu and C. Yang, *Environ. Sci. Pollut. Res.*, **26**(6), 5944 (2019).
11. C. He, J. Qu, Z. Yu, D. Chen, T. Su, L. He, Z. Zhao, C. Zhou, P. Hong and Y. Li, *Nanomaterials*, **9**(7), 953 (2019).
12. J. Chen, Y. Cai, M. Clark and Y. Yu, *PLoS One*, **8**(4), e60243 (2013).
13. W. You, M. Hong, H. Zhang, Q. Wu, Z. Zhuang and Y. Yu, *Phys. Chem. Chem. Phys.*, **18**(23), 15564 (2016).
14. M. Mariana, A.K. H.P.S., E. Mistar, E. B. Yahya, T. Alfatah, M. Danish and M. Amayreh, *J. Water Process Eng.*, **43**, 102221 (2021).
15. A. A. Aryee, F. M. Mpatani, A. N. Kani, E. Dovi, R. Han, Z. Li and L. Qu, *J. Clean. Prod.*, **310**, 127502 (2021).
16. S. Bao, W. Yang, Y. Wang, Y. Yu, Y. Sun and K. Li, *Chem. Eng. J.*, **399**, 125762 (2020).
17. C.-W. Cho, S. B. Kang, S. Kim, Y.-S. Yun and S. W. Won, *Chem. Eng. J.*, **302**, 545 (2016).
18. X. Tian, W. Wang, Y. Wang, S. Komarneni and C. Yang, *Micropor. Mesopor. Mater.*, **207**, 46 (2015).
19. S. Nayab, A. Farrukh, Z. Oluz, E. l. Tuncel, S. R. Tariq, H. u. Rahman, K. Kirchhoff, H. Duran and B. Yameen, *ACS Appl. Mater. Interfaces*, **6**(6), 4408 (2014).
20. Z. Wang, S. B. Kang and S. W. Won, *J. Environ. Chem. Eng.*, **9**(2), 105058 (2021).
21. H. A. Choi, H. N. Park and S. W. Won, *J. Environ. Manage.*, **204**, 200 (2017).
22. S. B. Kang, Z. Wang and S. W. Won, *Chem. Eng. Trans.*, **78**, 205 (2020).
23. K. M. Kim, Z. Wang, S. B. Kang and S. W. Won, *Korean J. Chem. Eng.*, **36**(9), 1455 (2019).
24. H. Nebel, M. Neumann, C. Mayer and M. Epple, *Inorg. Chem.*, **47**(17), 7874 (2008).
25. J. Wang, Y. He, Y. Yang, W. Xie and X. Ling, *Physicochem. Probl. Miner. Process.*, **53**(1), 227 (2017).
26. K. Baltakys, R. Jauberthie, R. Siauciunas and R. Kaminskas, *Mater. Sci.-Pol.*, **25**(3), 663 (2007).
27. S. W. Won, J. Park, J. Mao and Y.-S. Yun, *Bioresour. Technol.*, **102**(4), 3888 (2011).
28. T. Sakpal, A. Kumar, S. Kamble and R. Kumar, *Indian J. Chem.*, **51A**, 1214 (2012).
29. D. Zhang, H. E. Hegab, Y. Lvov, L. D. Snow and J. Palmer, *SpringerPlus*, **5**(1), 1 (2016).
30. D. Render, T. Samuel, H. King, M. Vig, S. Jeelani, R. J. Babu and V. Rangari, *J. Nanomater.*, **2016**, 3170248 (2016).
31. M. Zhang and J. Chang, *Ultrason. Sonochem.*, **17**(5), 789 (2010).
32. S. Sanna, W. G. Schmidt and P. Thissen, *J. Phys. Chem. C*, **118**(15), 8007 (2014).
33. K. Halubek-Gluchowska, D. Szymański, T. N. L. Tran, M. Ferrari and A. Lukowiak, *Materials*, **14**(4), 937 (2021).
34. M. Bouatrous, F. Bouzerara, A. K. Bhakta, F. Delobel, J. Delhalle and Z. Mekhalif, *Ceram. Int.*, **46**(8), 12618 (2020).
35. K. S. Sing and R. T. Williams, *Adsorpt. Sci. Technol.*, **22**(10), 773 (2004).
36. W. Guan, F. Ji, Q. Chen, P. Yan and L. Pei, *Materials*, **6**(7), 2846 (2013).
37. S.-C. Wu, H.-C. Hsu, Y.-N. Wu and W.-F. Ho, *Mater. Charact.*, **62**(12), 1180 (2011).
38. R. Xing, Y. Qin, X. Guan, S. Liu, H. Yu and P. Li, *Egypt. J. Aquat. Res.*, **39**(2), 83 (2013).
39. M. Huerta-Fontela, M. T. Galceran and F. Ventura, *Water Res.*, **45**(3), 1432 (2011).
40. M. H. Kim, C.-H. Hwang, S. B. Kang, S. Kim, S. W. Park, Y.-S. Yun and S. W. Won, *Chem. Eng. J.*, **280**, 18 (2015).
41. X. Zhao, X. Wang and T. Lou, *J. Hazard. Mater.*, **403**, 124054 (2021).
42. S. Y. Kazemi, P. Biparva and E. Ashtiani, *Ecol. Eng.*, **88**, 82 (2016).
43. M. Shirzad-Siboni, A. Khataee and S. W. Joo, *J. Ind. Eng. Chem.*, **20**(2), 610 (2014).
44. W. T. Tsai, K. J. Hsien, H. C. Hsu, C. M. Lin, K. Y. Lin and C. H. Chiu, *Bioresour. Technol.*, **99**(6), 1623 (2008).
45. S. Iftekhar, D. L. Ramasamy, V. Srivastava, M. B. Asif and M. Sillanpaa, *Chemosphere*, **204**, 413 (2018).
46. S. B. Kang, Z. Wang and S. W. Won, *Korean J. Chem. Eng.*, **38**(3), 523 (2021).